Biofouling characteristics of reverse osmosis membranes during dyeing wastewater desalination

Jianhong Shi[a,b], Yinglong Su[a,b], Chongxin Du[a,b], Bing Xie[a,b,*]

[a]*Key Laboratory of Urbanization and Ecological Restoration of Shanghai, School of Ecology and Environmental Science, East China Normal University, Shanghai 200241, China, Tel. +86 021 54341276; emails: bxie@des.ecnu.edu.cn (B. Xie) shijh910204@163.com (J. Shi), lydsyl@126.com (Y. Su), 616537532@qq.com (C. Du)*
[b]*Shanghai Institute of Pollution Control and Ecological Security, Shanghai 200092, China*

ABSTRACT

Membrane biofouling is an unevadable problem that occurr during the reverse osmosis (RO) desalination of dyeing wastewater; therefore, it is necessary to minutely understand biofouling characteristics of RO membranes to effectively hinder the fouling. In this study, two sets of laboratory-scale desalination systems of biologically treated dyeing wastewater were operated, respectively, for 10 and 30 d, and the performance and biofouling of RO membrane were investigated. The obvious decrease of permeate flux after 10 d of operation reflected a more serious membrane fouling. The analysis on surface morphology, foulant characteristics, and active biomass of membrane fouling layer exemplified that biofouling was perhaps responsible for the permeate flux decline, and the fouling was more serious after operation of 30 d than that of 10 d. Further, bacterial community of biofilm showed that Proteobacteria was the most predominant, followed by Firmicutes and Bacteroidete. The relative abundance of γ-Proteobacteria significantly decreased and that of α-Proteobacteria, Clostridia, and Sphingobacteria increased with operation time, which seemed to facilitate the more developed/mature biofilm formation. The results would provide fundamental information for effective strategy on prevention and control of membrane biofouling during RO desalination of dyeing wastewater.

Keywords: Dyeing wastewater; Reverse osmosis membrane; Biofouling; Bacterial community

1. Introduction

The dyeing process of textiles is characterized by high water consumption and wastewater generation [1]. Generated dyeing wastewater is difficult to realize the desalination and complete mineralization of refractory organic matter due to its high organic concentration and low degradability [2]. Thus, an effective technology of recovery and reuse of water coming from dyeing wastewater are needed urgently to reduce water consumption and minimize effluent discharge. In recent years, reverse osmosis (RO) membrane technology has been highlighted in reuse of effluents from textile industry with its outstanding attributes of high contaminant rejection, simple operation, and producing high-quality water [3–5]. Ciardelli et al. [6] has applied RO membrane technology after biological-sand filter and ultrafiltration (UF) to produce high-quality water being reused in dyeing processes.

However, membrane fouling poses a formidable challenge for the application of RO technology, which may result in the decline of membrane performance and limit the RO system efficiency [7,8]. The types of membrane fouling can be classified into colloidal fouling, inorganic/organic fouling, and biofouling [9]. Biofouling is one of the major concerns in the RO process [9,10], which has been observed within a first few hours of RO operation [11,12]. A complex sessile microbial community grows by deposition, attachment, and proliferation of microorganisms on the membrane surface to form a biofilm [13], causing an increase in hydraulic resistance, a

* Corresponding author.

severe decline in permeate flux, and a deterioration of system performance for RO membrane [14–17]. Once the biofilm is established, it is difficult to remove by treatment with a variety of chemical cleaning agents due to the protection provided by self-produced extracellular polymeric substances (EPS) [18,19]. Previous studies have reported that chemical treatment affected only the top biofilm surface, and sufficient bacteria remained on the membranes still could cause potential problem [19,20]. Given that biofouling is the most ubiquitous and recalcitrant, an in-depth analysis in microbial community of biofilm on the RO membrane would be useful for prevention and control of membrane biofouling and good performance maintenance of RO system. For the treatment of drinking water, seawater, or municipal wastewater effluents, previous studies have reported two major bacterial phyla, Proteobacteria and Bacteroidetes, which played a critical role in biofilm development on RO membrane [21–24]. Nevertheless, for RO desalination of dyeing wastewater, it is still necessary to further investigate biofilm composition at different operation time to better understand the membrane biofouling mechanisms.

The main objective of this study was to gain a better insight into the membrane biofouling characteristics in RO systems for dyeing wastewater desalination. To trace the changes occurring in the biofouling layer, diversity and bacterial community composition were assessed by high-throughput sequencing techniques. The fouled RO membranes were autopsied after operation for 10 and 30 d, and a comparative analysis of surface morphology, foulant characteristics, active biomass, diversity, and composition of bacterial communities was carried out.

2. Materials and methods

2.1. RO membrane unit operation and sample collection

The laboratory-scale RO desalination system was fed with UF permeate of biological-sand-treated dyeing wastewater. The spiral-wound aromatic polyamide composite RO membrane, YQS-4040 (Hydranautics, USA) with a filtration area of 7.2 m^2 (4-inch diameter), was used in this system. Two sets of RO unit were operated continuously with uniform operation conditions for 10 and 30 d at 25°C ± 2°C, respectively, with initial pressure of 0.6 MPa and the feed water flow rate of 0.3 m^3/h. The recovery of each RO unit was 50%. RO influent was characterized as chemical oxygen demand of 90–122 mg/L, pH of 6.8–8.0, conductivity of 2,200–3,000 μs/cm, total nitrogen of 24–36 mg/L, and total phosphorus of 2.5–3.2 mg/L. Permeate flux and salt rejection were monitored every 2 d. Salt rejection was calculated as follows:

$$\text{Salt rejection} = 100 \times \left(1 - \frac{\text{Conductivity}_{\text{permeates}}}{\text{Conductivity}_{\text{influent}}}\right)$$

At the end of each operation, RO membrane was autopsied within 24 h for surface morphology observation and foulant collection. The foulant samples in triplicate were collected from the inlet and outlet parts of fouled RO membranes by physical scrapping, which were nearer to RO influent and RO concentrate, respectively.

2.2. Fouling load analysis and loss on ignition test

Foulants were dried by lyophilization process, and recovered foulants were weighed. Mass per unit surface area of the fouled membrane was calculated as fouling load [22]. Lyophilized foulants were dried in 110°C to constant weight and then subjected to ignition at 550°C for 4 h in a muffle furnace. The residual and loss samples after ignition at 550°C represented inorganic and organic fractions, respectively [2]. The percentage of inorganic/organic fractions was calculated as weight of inorganic/organic fractions/constant weight × 100.

2.3. Bacterial cell counts

The foulants scrapped from the RO membrane surfaces were dissolved in sterilized phosphate buffer solution (PBS) with vortex shaking. Heterotrophic plate counts (HPC) and adenosine triphosphate (ATP) of the samples were immediately analyzed. HPC was calculated according to the International Standard [25]. All samples were properly diluted in sterilized PBS, and then the diluted samples were evenly coated on Luria-Bertani agar plates. Plates were put into a constant temperature incubator (25°C) for 7 d to obtain colony counts of 30–300 per plate. ATP was measured using the G819A BacTiter-Glo Microbial Cell Viability Assay kit (USA) according to the manufacturer's guidelines. The luminescence of samples was read in an MD SpectraMax M5 multifunctional microplate reader (Molecular Devices, USA).

2.4. DNA extraction and Illumina high-throughput sequencing

The total genomic DNA was extracted from foulant deposited at the inlet and outlet parts of fouled RO membranes in triplicate using AZecoTM Soil DNA MiniPrep (Azanno Biotech, China) according to the manufacturer's protocols. Triplicate total genomic DNA was homogenized together to average out bias sampling and extraction. DNA concentrations and purity were quantified by agarose electrophoresis, and Qubit 2.0 DNA kit (Sangon, China) was used to determine genomic DNA for polymerase chain reaction (PCR) reaction. About 420 pb hypervariable V3–V4 region of the bacterial 16S ribosomal ribonucleic acid (rRNA) gene was PCR amplified using the primer (515F/806R) [26]. The PCR reactions were conducted in a 50-μL mixture including 5 μL of 10× PCR buffer, 0.5 μL of deoxynucleoside triphosphate (10 mM), 10 ng of genomic DNA, 1 μL of each primer (50 μM), and 0.5 μL of Platium Taq (5 U/μL). The PCR amplification procedure was as follows: initial denaturation step of 2 min at 95°C, followed by 25 cycles (95°C for 30 s, 55°C for 30 s, 72°C for 30 s), and a final extension at 72°C for 5 min [27]. The PCR products were checked by 1.0% agarose gel electrophoresis and then were subjected to library preparation using Illumina TruSeq DNA PCR-free sample preparation kit according to the manufacturer's instructions. Pyrosequencing was conducted on the Illumina Miseq 2,000 platform (PersonalBio, Shanghai) to assess the diversity and relative abundances of bacteria in all samples. The raw sequences were processed using the Pipeline Initial Process tool of the Ribosomal Database Project (RDP) to sort based on the specific barcodes. The adapters and primers were trimmed using Trimmomatic software (v 0.33), and the sequences containing ambiguous 'N', low-quality tags,

chimeras, and shorter than 200 bp in length were removed by Quantitative Insights into Microbial Ecology (v 1.8.0) [28]. The quality-filtered sequences were then checked using Mothur (http://www.mothur.org) and clustered into operational taxonomic unit (OTUs) by USEARCH method at a 97% identity threshold [20]. The resulting OTU representative sequences were submitted to Greengenes Database (http://greengenes.secondgenome.com/) with RDP Classifier with a confidence threshold of 0.80. Shannon-Weaver index for diversity estimation and Chao1 estimator for species richness were calculated across these samples [29]. All sequences used in this study were submitted to the National Center for Biotechnology Information (Accession Number: SRP166765).

2.5. Analytical methods

Conductivity was measured by a DDS-307A conductivity meter (China). The surface morphology of fouled RO membranes was observed using scanning electron microscopy (SEM) (Phenom G2 Pro, the Netherlands). Principal component analysis (PCA) was performed to identify clusters of bacteria in the different samples. One-way analysis of variance was applied to test for significant differences of results, and P value <0.05 was considered to be statistically significant. All the analyses were performed with statistic package for the social science (SPSS) 22.0 Statistics (IBM Corp., USA).

3. Results and discussion

3.1. Change of membrane performance during RO desalination

Membrane fouling can result in a decrease of permeate flux, which has been generally used as an indicative parameter to evaluate the fouling in various studies [2,30]. In this study, a gradual decrease in the permeate flux was observed with a reduction of permeability of 42.8% until the end of operation, and a more serious decline occurred after 10 d accounting for 83.4% of the overall decline (Fig. 1). The results indicated that the RO membranes had a relatively moderate fouling within 10 d of operation, and the fouling

were significantly increased from 10 to 30 d. In contrast with the obvious decrease in permeate flux, a relatively steady salt rejection was measured, which exhibited the great capability of RO membrane separation for wastewater desalination, even upon moderate fouling.

3.2. Surface morphology and foulant characteristics of RO membrane fouling layer

The surface morphology of autopsied membranes at the end of operation was analyzed with SEM technique as shown in Fig. 2(a). It was found that the surface of RO membrane was relatively rough and scattered after 10 d, but a densely packed and homogeneous fouling layer was visualized on the membrane surface, which was colonized by a large number of microbes after 30 d. SEM analysis directly showed the fouled RO membrane and exemplified the presence of more serious fouling after 30 d of operation to some extent. The findings seemed to be consistent with the decrease of permeate flux.

The analysis of fouling load was performed to quantitatively evaluate membrane fouling corresponding to the qualitative SEM data. Both the fouling loads of the inlet part of RO membranes at two different time scales (i.e., 0.62 ± 0.07 g/m^2 for 10 d and 1.56 ± 0.14 g/m^2 for 30 d) were higher than those of outlet part of the RO membranes (i.e., 0.31 ± 0.01 g/m^2 for 10 d and 0.93 ± 0.09 g/m^2 for 30 d) (Fig. 2(b)), suggesting higher potential of the fouling load at the inlet part of RO membranes. Furthermore, fouling loads significantly increased from 10 to 30 d, which reconfirmed the occurrence of rapidly increasing fouling on the RO membranes with operation time.

The fouling load was further characterized as organic and inorganic fractions by loss on ignition test. As shown in Fig. 2(c), the average percentage of organic and inorganic fractions on the RO membranes after 10 d were $85.6\% \pm 2.5\%$ and $14.4\% \pm 2.3\%$ for the inlet part and $88.1\% \pm 3.9\%$ and $11.9\% \pm 3.5\%$ for the outlet part and those after 30 d were $91.4\% \pm 4.4\%$ and $8.6\% \pm 2.1\%$ for the inlet part and $94.3\% \pm 3.6\%$ and $5.7\% \pm 1.5\%$ for the outlet part. The results proved that the higher fouling load on the RO membrane was mainly attributed to the accumulation of organic foulants. Besides, the proportion of organic foulants remarkably increased ($P < 0.05$) with time. Previous studies have reported that initial organic matter adhesion could accelerate the bacterial accumulation on RO membrane surface and eventually the formation of biological fouling [19,31,32]. In our study, substantial bacterial aggregation was also visualized on the fouled membrane by SEM. It is well known that bacteria can produce a large number of EPS by metabolism, being mainly composed of polysaccharides and proteins [18]. Therefore, the increased proportion of organic foulants due to organic matter adsorbed on the membrane surface led to a large growth of bacteria and subsequent accumulation of biopolymer matrix.

3.3. Biomass characterization of the RO membrane fouling layer

In this study, ATP and HPC in the RO membrane fouling layer were measured as an indicator of active biomass [2,20,33] (Fig. 3(a)). The ATP contents at the inlet and outlet parts of RO membranes were 982 ± 185 pg/cm^2 and
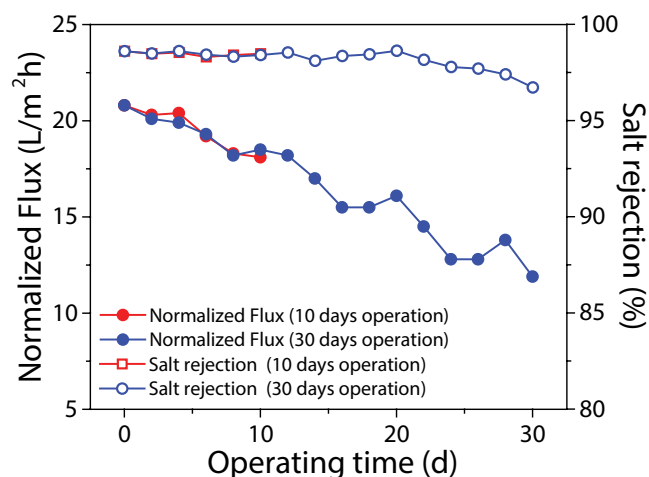
Fig. 1. Changes in normalized permeate flux (at 0.6 MPa, 25°C ± 2°C) and salt rejection of the membranes during RO desalination of dyeing wastewater.
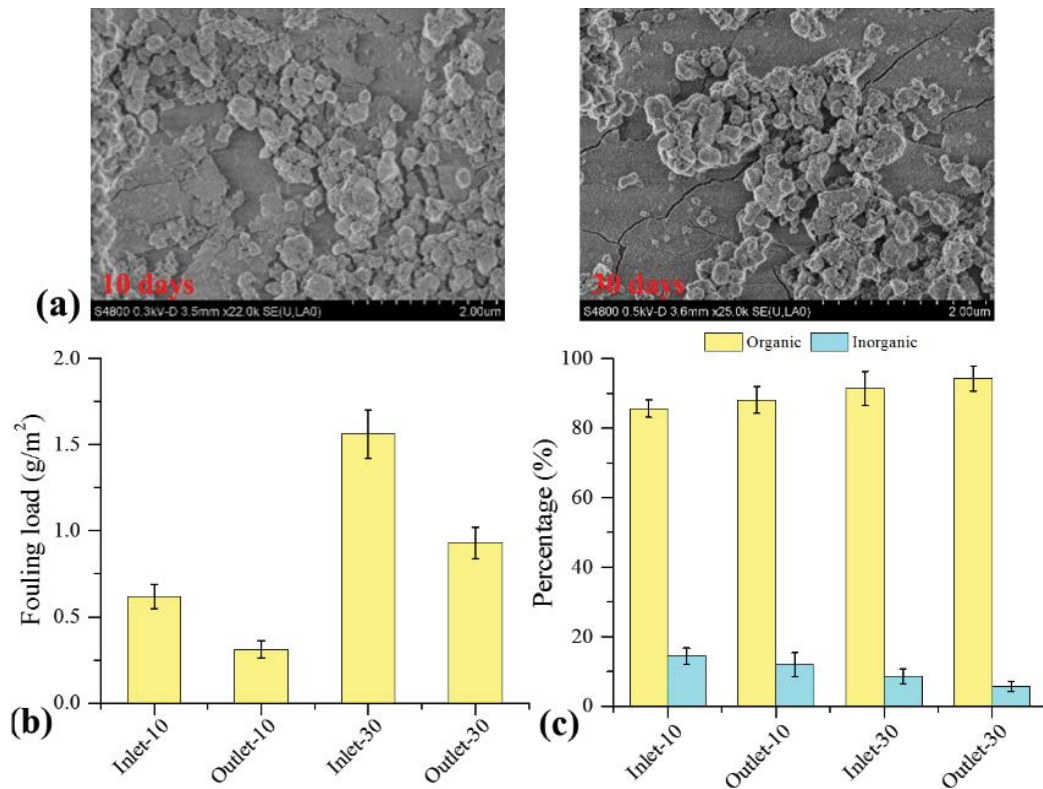
Fig. 2. Surface morphology and foulant characteristics of fouling layer on the RO membrane for dyeing wastewater desalination after operation for 10 and 30 d: SEM images (a), fouling load (b), and the percentage of organic and inorganic fractions of foulants (c), Inlet-10, Inlet-30, Outlet-10, and Outlet-30 represented the samples collected from the inlet and outlet parts of the RO membrane after operation for 10 and 30 d, respectively.
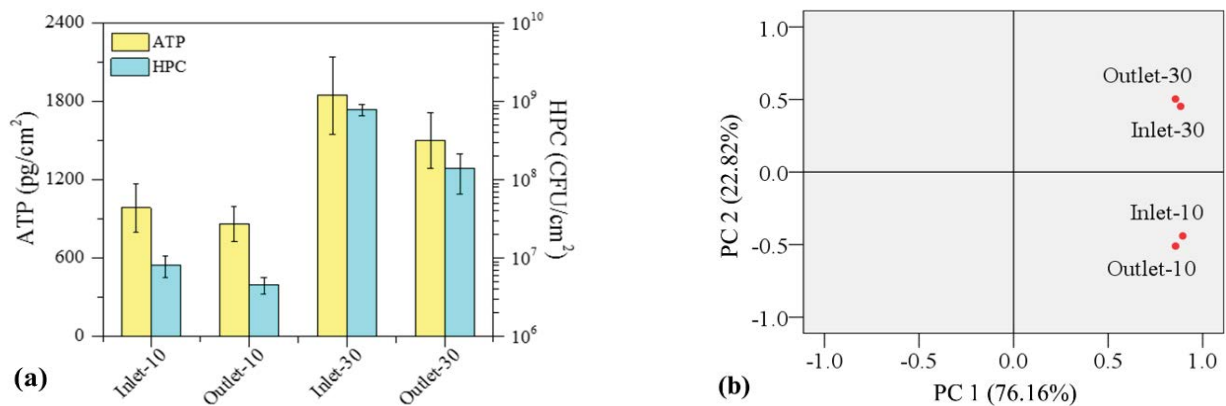
Fig. 3. The contents of active biomass (HPC and ATP) (a) and principal component analysis (PCA) of the bacterial community (b) in the RO membrane biofilm after operation for 10 and 30 d.

862 ± 234 pg/cm^2 for 10 d operation and $1,845 \pm 296$ pg/cm^2 and $1,497 \pm 376$ pg/cm^2 for 30 d operation, respectively. HPC at the inlet and outlet parts of RO membranes at two different scales were $8.2 \pm 2.5 \times 10^6$ CFU/cm^2 and $4.6 \pm 2.1 \times 10^6$ CFU/cm^2 for 10 d and $7.5 \pm 1.9 \times 10^8$ CFU/cm^2 and $9.4 \pm 2.8 \times 10^7$ CFU/cm^2 for 30 d. The inlet part of RO membrane has relatively higher active biomass than those at the outlet part of RO membrane, which supported higher potential of fouling formed on the inlet part compared with the outlet part of RO membranes.

Furthermore, the RO membrane after 30 d exhibited significantly higher ($P < 0.05$) active biomass than that after 10 d, demonstrating more developed biofilm or biofouling forming on the RO membrane. It can be speculated therefore that more severe biofouling from 10 d onwards played a major role in causing the significant decrease of permeate flux. On one hand, the aggregation of numerous bacterial cells on the membrane surface may decrease permeate flux by a biofilm-enhanced osmotic pressure mechanism [9]. On

the other hand, the bacterial cells were supposed to produce EPS [34], which induced membrane permeability decline by increasing the hydraulic resistance to permeate flow [35].

3.4. Taxonomic diversity and bacterial community composition of biofilm in the RO membrane fouling layer

The bacterial diversity in the RO membrane biofilm was evaluated using the Chao I index and the Shannon-Weaver diversity index (Table 1). The Chao I index and the Shannon-Weaver diversity index showed the same trend, which decreased from the inlet to outlet part of RO membrane and increased from 10 to 30 d. The results indicated that the diversity of the bacterial communities at the inlet of RO membrane was higher than that at the outlet of the RO membrane; further, the diversity of the bacterial communities increased with the biofilm age. Briones and Raskin proved that a highly diverse bacterial ecosystem was beneficial to community stability and functional resistance to perturbation and stress [36].

To better understand the dynamic change of biofouling, bacterial community composition of biofilm in the RO membrane fouling layer was detected at the inlet and outlet parts of RO membrane at two different time scales. PCA was used to cluster-analyze the bacterial community in the different samples, revealing that bacterial communities at the inlet and outlet of RO membrane were similar to each other, while there was a substantial difference between bacterial communities after operation for 10 and 30 d (Fig. 3(b)). The results supported RO membrane biofouling was a complex and dynamic phenomenon, and the relative abundance of bacterial population changed with the biofilm age as also suggested previously [37]. The development of the unique bacterial community on the RO membrane might be related to biofilm development traits.

Detailed composition of bacterial communities of biofilm in 10- and 30-d samples are shown in Fig. 4, regardless of that at the inlet and outlet parts of RO membrane. The bacterial communities were dominated by Proteobacteria (83.2% ± 5.6%) followed by Firmicutes (7.2% ± 2.3%) and Bacteroidetes (5.8% ± 2.5%) after 10 d of

operation. Within the dominant phylum, the subclasses γ-, β-, α-Proteobacteria ruled the community with relative abundance of 50.5% ± 3.1%, 20.2% ± 0.6%, and 9.7% ± 1.2%, respectively. The γ-Proteobacteria were dominated by the orders Enterobacteriales (25.4% ± 3.3%), Aeromonadales (12.5% ± 2.4%), Pseudomonadales (9.8% ± 1.2%), and Xanthomonadales (2.1% ± 0.7%). Most β-Proteobacteria belonged to the order Burkholderiales with relative abundance of 17.5% ± 2.3%, while α-Proteobacteria were represented by the orders Sphingomonadales (5.9% ± 0.8%) and Rhizobiales (3.1% ± 1.3%). The Firmicutes phylum was composed mainly of the classes Clostridia (4.2% ± 0.9%) and Bacilli (2.1% ± 0.5%), and Bacteroidetes phylum was dominated by the class Sphingobacteria (4.9% ± 0.6%).

After 30 d of operation, an obvious decrease in the relative abundance of Proteobacteria (67.3% ± 5.6%) in the RO membrane biofilm was found; however, the relative abundance of Firmicutes and Bacteroidetes increased to 12.3% ± 1.8% and 15.7% ± 2.9%, respectively. At the class level, the relative abundance of γ- Proteobacteria reduced to 30.1% ± 3.6% while the relative abundance of α-Proteobacteria increased to 15.8% ± 2.2%. β-Proteobacteria (18.1% ± 2.5%) exhibited the highest community structure stability. At the order level, Sphingomonadales and Rhizobiales showed an increasing trend with the relative abundance of 11.8% ± 1.2% and 9.3% ± 1.4%, respectively, and Enterobacteriales, Aeromonadales, Pseudomonadales, and Xanthomonadales decreased to 14.8% ± 1.3%, 6.2% ± 0.9%, 2.8% ± 0.3%, and 1.7% ± 0.08%, respectively. The relative abundance of Burkholderiales was 17.4% ± 2.1% and showed slight change.

Table 1
Diversity indices of bacterial phylotypes

Parameter	Chao I index	Shannon index
Inlet-10	1,842 ± 595	7.5 ± 0.6
Outlet-10	1,723 ± 347	6.8 ± 0.3
Inlet-30	2,846 ± 498	8.6 ± 0.5
Outlet-30	2,539 ± 602	7.9 ± 0.2
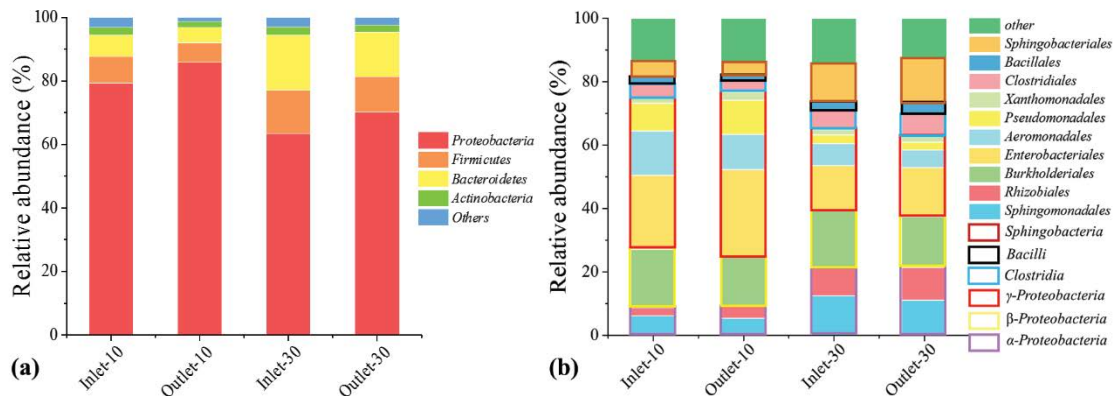
Fig. 4. The bacterial community compositions in the RO membrane biofilm after operation for 10 and 30 d at the phylum level (a) and class and order levels (b). Phylum, class, and order in all samples with greater than 1% abundance are listed. "Others" indicates the sum of unidentified bacteria and other minor bacteria.

In addition, the relative abundance of classes Clostridia and Bacilli within Firmicutes phylum increased to 7.1% ± 0.9% and 3.3% ± 0.5%, respectively, and the predominant class Sphingobacteria within Bacteroidetes phylum increased to 13.5% ± 1.4%.

3.5. Implications of dominant bacterial population for biofilm formation and development

In our study, the Proteobacterial phylum was predominant in the RO membrane biofilm in both 10- and 30-d samples. Their class, γ-, β-, and α-Proteobacteria, played a dramatic role in biofilm formation and development on the RO membranes since they made up the majority of the Proteobacteria groups, which were in accordance with previous reports [29,38]. This profile appeared to be associated with their capability to colonize on the membrane surface, degrade a broad range of synthetic and natural organic compounds, and propagate under oligotrophic conditions [39–41]. γ-Proteobacteria were the most dominant Proteobacterial group, and significant decline was observed from 10 to 30 d. Hörsch et al. also emphasized the importance of γ-Proteobacteria as initial colonizers at primary biofilm by an attachment mechanism [21]. We speculate therefore that the predominance of γ-Proteobacteria will be weaken with biofilm age. However, the α-Proteobacteria, dominated by the orders Rhizobiales and Sphingomonadales, showed noticeable growth in the RO membrane biofilm from 10 to 30 d, indicating Rhizobiales and Sphingomonadales played an important role in more mature biofilm on the RO membrane fed by dyeing effluent wastewater. The Rhizobiales and Sphingomonadales have been reported to produce glycosphingolipids, which are of importance in bacteria's initial colonization of RO membranes and in production of exopolysaccharides during bacterial biofilm maturation [29]. Additionally, the preponderance of β-Proteobacteria in the biofilm of nanofiltration membrane fed by tertiary effluent wastewater generated in a continuous flow membrane bioreactor has been reported by Ivnitsky et al. [41]. In our study, β-Proteobacteria, most of which belonged to the order Burkholderiales, exhibited relatively stable abundance during the entire operating period, being indicative of a major contribution of β-Proteobacteria (or Burkholderiales) during the whole biofilm development. In addition to Proteobacteria, both Firmicutes and Bacteroidetes, especially their subclasses Clostridia and Sphingobacteria, respectively, exhibited increased advantage with biofilm age. According to Belila et al. [42], Bacteroidetes could be well adapted to grow on membrane surfaces and play a role in degrading biopolymers.

Taken together, the dominant Proteobacteria, Firmicutes, and Bacteroidetes were crucial to the formation and development of biofilm in the RO membrane fouling layer during dyeing wastewater desalination. Further, considerable changes in bacterial community of biofilm could be found with operation time, which was perhaps related to more dramatic deterioration of membrane performance. The dynamic change of bacterial community of biofilm on RO membranes promoted the further understanding of biofouling phenomenon, which would provide useful insights into the rational application of cleaning and disinfecting protocols to hinder biofouling.

4. Conclusion

Biofouling on the RO membrane was significantly increased with operation time, which was mainly responsible for the dramatic deterioration of permeate flux during dyeing wastewater desalination. The bacterial community of biofilm were dominated by Proteobacteria followed by Firmicutes and Bacteroidetes after operation for 10 and 30 d. γ-Proteobacteria was the most dominant Proteobacterial group, and the relative abundance of that significantly decreased with biofilm age. α-Proteobacteria, Clostridia, and Sphingobacteria showed marked increase with biofilm age, which probably contributes to the more developed/mature biofilm formation.

References

[1] Z. Yin, C. Yang, C. Long, A. Li, Effect of integrated pretreatment technologies on RO membrane fouling for treating textile secondary effluent: laboratory and pilot-scale experiments, Chem. Eng. J., 332 (2018) 109–117.

[2] Y. Tan, L. Sun, B. Li, X. Zhao, T. Yu, N. Ikuno, K. Ishii, H. Hu, Fouling characteristics and fouling control of reverse osmosis membranes for desalination of dyeing wastewater with high chemical oxygen demand, Desalination, 419 (2017) 1–7.

[3] I.C. Kim, K.H. Lee, Dyeing process wastewater treatment using fouling resistant nanofiltration and reverse osmosis membranes, Desalination, 192 (2006) 246–251.

[4] J. Dasgupta, J. Sikder, S. Chakraborty, S. Curcio, E. Drioli, Remediation of textile effluents by membrane based treatment techniques: a state of the art review, J. Environ. Manage., 147 (2015) 55–72.

[5] M.A. Al-Obaidi, J.P. Li, C. Kara-Zaïtri, I.M. Mujtaba, Optimisation of reverse osmosis based wastewater treatment system for the removal of chlorophenol using genetic algorithms, Chem. Eng. J., 316 (2017) 91–100.

[6] G. Ciardelli, L. Corsi, M. Marcucci, Membrane separation for wastewater reuse in the textile industry, Resour. Conserv. Recycl., 31 (2001) 189–197.

[7] M. Al-Ahmad, F.A.A. Aleem, A. Mutiri, A. Ubaisy, Biofouling in RO membrane systems part 1: fundamentals and control, Desalination, 132 (2000) 173–179.

[8] A. Lerch, N. Siebdrath, P. Berg, M. Heijnen, V. Gitis, W. Uhl, Fouling minimised reclamation of secondary effluents with reverse osmosis (ReSeRo), Desal. Wat. Treat., 42 (2012) 181–188.

[9] M. Herzberg, M. Elimelech, Biofouling of reverse osmosis membranes: role of biofilm-enhanced osmotic pressure, J. Membr. Sci., 295 (2007) 11–20.

[10] M. Kumar, S.S. Adham, W.R. Pearce, Investigation of seawater reverse osmosis fouling and its relationship to pretreatment type, Environ. Sci. Technol., 40 (2006) 2037–2044.

[11] W. Lee, C.H. Ahn, S. Hong, S. Kim, S. Lee, Y. Baek, J. Yoon, Evaluation of surface properties of reverse osmosis membranes on the initial biofouling stages under no filtration condition, J. Membr. Sci., 351 (2010) 112–122.

[12] C.L. Chen, W.T. Liu, M.L. Chong, M.T. Wong, S.L. Ong, H. Seah, W.J. Ng, Community structure of microbial biofilms associated with membrane-based water purification processes as revealed using a polyphasic approach, Appl. Microbiol. Biotechnol., 63 (2004) 466–473.

[13] C.M. Pang, P. Hong, H. Guo, W.T. Liu, Biofilm formation characteristics of bacterial isolates retrieved from a reverse osmosis membrane, Environ. Sci. Technol., 39 (2005) 7541–7550.

[14] E.M. Hoek, M. Elimelech, Cake-enhanced concentration polarization: a new fouling mechanism for salt-rejecting membranes, Environ. Sci. Technol., 37 (2003) 5581–5588.

[15] L. Bereschenko, G. Heilig, M. Nederlof, M.A. Van Loosdrecht, G. Euverink, Molecular characterization of the bacterial communities in the different compartments of a full-scale reverse-osmosis water purification plant, Appl. Environ. Microbiol., 74 (2008) 5297–5304.

[16] L.N. Huang, H.D. Wever, L. Diels, Diverse and distinct bacterial communities induced biofilm fouling in membrane bioreactors operated under different conditions, Environ. Sci. Technol., 42 (2008) 8360–8366.

[17] S.R. Suwarno, X. Chen, T.H. Chong, V.L. Puspitasari, D. Mcdougald, Y. Cohen, S.A. Rice, A.G. Fane, The impact of flux and spacers on biofilm development on reverse osmosis membranes, J. Membr. Sci., 405–406 (2012) 219–232.

[18] H.C. Flemming, J. Wingender, The biofilm matrix, Nat. Rev. Microbiol., 8 (2010) 623–633.

[19] L.A. Bereschenko, H. Prummel, G.J.W. Euverink, A.J.M. Stams, M.C.M. van Loosdrecht, Effect of conventional chemical treatment on the microbial population in a biofouling layer of reverse osmosis systems, Water Res., 45 (2011) 405–416.

[20] T. Yu, L. Meng, Q.-B. Zhao, Y. Shi, H.-Y. Hu, Y. Lu, Effects of chemical cleaning on RO membrane inorganic, organic and microbial foulant removal in a full-scale plant for municipal wastewater reclamation, Water Res., 113 (2017) 1–10.

[21] P. Hörsch, A. Gorenflo, C. Fuder, A. Deleage, F. Frimmel, Biofouling of ultra-and nanofiltration membranes for drinking water treatment characterized by fluorescence in situ hybridization (FISH), Desalination, 172 (2005) 41–52.

[22] M.T. Khan, M. Busch, V.G. Molina, A.H. Emwas, C. Aubry, J.P. Croue, How different is the composition of the fouling layer of wastewater reuse and seawater desalination RO membranes?, Water Res., 59 (2014) 271–282.

[23] T. Baba, R. Matsumoto, N. Yamaguchi, M. Nasu, Bacterial population dynamics in a reverse-osmosis water purification system determined by fluorescent staining and PCR denaturing gradient gel electrophoresis, Microbes Environ., 24 (2009) 163–167.

[24] C. Ayache, C. Manes, M. Pidou, J.P. Croue, W. Gernjak, Microbial community analysis of fouled reverse osmosis membranes used in water recycling, Water Res., 47 (2013) 3291–3299.

[25] Water Quality-Enumeration of Culturable Microorganisms-Colony Count by Inoculation in a Nutrient Agar Culture Medium, ISO6222, 1999.

[26] Y. Su, J. Wang, Z. Huang, B. Xie, On-site removal of antibiotics and antibiotic resistance genes from leachate by aged refuse bioreactor: effects of microbial community and operational parameters, Chemosphere, 178 (2017) 486.

[27] H. Zhou, D. Li, F.Y. Tam, X. Jiang, H. Zhang, H. Sheng, J. Qin, X. Liu, F. Zou, BIPES, a cost-effective high-throughput method for assessing microbial diversity, ISME J., 5 (2010) 741–749.

[28] M.J. Claesson, O. O'Sullivan, Q. Wang, J. Nikkilä, J.R. Marchesi, H. Smidt, W.M. de Vos, R.P. Ross, P.W. O'Toole, Comparative analysis of pyrosequencing and a phylogenetic microarray for exploring microbial community structures in the human distal intestine, PLoS One, 4 (2009) e6669.

[29] A.A. Ashhab, M. Herzberg, O. Gillor, Biofouling of reverse-osmosis membranes during tertiary wastewater desalination: microbial community composition, Water Res., 50 (2014) 341–349.

[30] T.H. Chong, F.S. Wong, A.G. Fane, The effect of imposed flux on biofouling in reverse osmosis: role of concentration polarisation and biofilm enhanced osmotic pressure phenomena, J. Membr. Sci., 325 (2008) 840–850.

[31] A. Matin, Z. Khan, S.M.J. Zaidi, M.C. Boyce, Biofouling in reverse osmosis membranes for seawater desalination: phenomena and prevention, Desalination, 281 (2011) 1–16.

[32] S. Jeong, S.J. Kim, H.K. Lan, M.S. Shin, S. Vigneswaran, T.V. Nguyen, I.S. Kim, Foulant analysis of a reverse osmosis membrane used pretreated seawater, J. Membr. Sci., 428 (2013) 434–444.

[33] M.T. Khan, C.-L. de O. Manes, C. Aubry, J.P. Croue, Source water quality shaping different fouling scenarios in a full-scale desalination plant at the Red Sea, Water Res., 47 (2013) 558–568.

[34] M.M. Ramsey, M. Whiteley, Pseudomonas aeruginosa attachment and biofilm development in dynamic environments, Mol. Microbiol., 53 (2010) 1075–1087.

[35] M. Herzberg, S. Kang, M. Elimelech, Role of extracellular polymeric substances (EPS) in biofouling of reverse osmosis membranes, Environ. Sci. Technol., 43 (2009) 4393–4398.

[36] A. Briones, L. Raskin, Diversity and dynamics of microbial communities in engineered environments and their implications for process stability, Curr. Opin. Biotechnol., 14 (2003) 270–276.

[37] M.T. Khan, C.-L. de O. Manes, C. Aubry, L. Gutierrez, J.P. Croue, Kinetic study of seawater reverse osmosis membrane fouling, Environ. Sci. Technol., 47 (2013) 10884–10894.

[38] L.A. Bereschenko, A.J.M. Stams, G.J.W. Euverink, M.C.M. van Loosdrecht, Biofilm formation on reverse osmosis membranes is initiated and dominated by Sphingomonas spp, Appl. Environ. Microbiol., 76 (2010) 2623–2632.

[39] H.S. Vrouwenvelder, J.A.M.V. Paassen, H.C. Folmer, J.A.M.H. Hofman, M.M. Nederlof, D.V.D. Kooij, Biofouling of membranes for drinking water production, Desalination, 118 (1998) 157–166.

[40] M.I. Sarro, A.M. Garcia, D.A. Moreno, Biofilm formation in spent nuclear fuel pools and bioremediation of radioactive water, Int. Microbiol., 8 (2005) 223–230.

[41] H. Ivnitsky, I. Katz, D. Minz, G. Volvovic, E. Shimoni, E. Kesselman, R. Semiat, C.G. Dosoretz, Bacterial community composition and structure of biofilms developing on nanofiltration membranes applied to wastewater treatment, Water Res., 41 (2007) 3924–3935.

[42] A. Belila, J. El-Chakhtoura, N. Otaibi, G. Muyzer, G. Gonzalez-Gil, P.E. Saikaly, M.C.M. van Loosdrecht, J.S. Vrouwenvelder, Bacterial community structure and variation in a full-scale seawater desalination plant for drinking water production, Water Res., 94 (2016) 62–72.